Preparation And Properties of Electroless Cu/Ni Composite Materials Based On Wood

Yanfei Pan (panyanfeiz@imau.edu.cn)
Inner Mongolia Agricultural University https://orcid.org/0000-0003-0130-1115
Qiang GUO
Inner Mongolia Agricultural University
Dingwen YIN
Inner Mongolia Agricultural University
Mayin DAI
Inner Mongolia Agricultural University
Xiaofang YU
Inner Mongolia Agricultural University
Yinan HAO
Inner Mongolia Agricultural University
Jintian HUANG
Inner Mongolia Agricultural University https://orcid.org/0000-0002-3770-5405

Research Article

Keywords: Wood, Electroless Cu/Ni, Surface roughness, Conductivity, Electromagnetic shielding

Posted Date: September 9th, 2021

DOI: https://doi.org/10.21203/rs.3.rs-884930/v1

Abstract

The changes of properties of wood-based Cu-Ni composites were studied via electroless Cu and Ni on wood surface to obtain Cu-Ni multilayer composites with excellent properties. The surface and interface morphology of the composite coatings were investigated via laser confocal microscopy and scanning electron microscope (SEM). The crystal structure was characterized by XRD. The hydrophobic properties of the composite coatings were tested via contact angle meter. The surface conductivity of composites was tested via four-probe. The results showed that the electrical conductivity of wood-based Cu-Ni composites was 2370.76 S/cm. The surface roughness was 9.99 μm and the thickness of uniform coating reached 157 μm via one time electroless Ni deposition and two times electroless Cu deposition. XRD analysis showed that the wood surface was uniformly covered with metal coating. The metal Cu and Ni were closely nested together to form a dense composite layer, and the composite material was light in weight. When the electroless Ni was 55 min, the contact angle could reach 123°, indicating that had best hydrophobicity. The average electromagnetic shielding effectiveness (EMSE) of Cu and Ni wood-based composites can reach 93.8 dB at L band ranging from 0.3×10^3 to 3.0×10^3 MHz) with a low thickness (157 μm), verified the multilayer composite materials can block over 99.99% of incident EM waves.

Introduction

With electronics technique developing rapidly, electromagnetic pollution has become the focus for people pay close attention to. Therefore, Wood-based metal functional composites are widely studied as superior electromagnetic shielding materials. Wood-based metal composites, as a kind of electromagnetic shielding material,were light weight, convenient to prepare and high shielding efficiency that have good development prospects. Wood-based metal functional composites first appeared in patents in the 1920s. The use of early wood-based metal functional composites is mainly based on its superior mechanical properties, many homes had used such composites by the 1960s [1]. In recent years, the research of wood-based metal functional composites mainly focuses on thermal conduction and electric conduction, which can be used as wood floor for geothermal heating [2]. Nano-Cu/ZnO coating wood matrix composites was prepared via magnetron sputtering method to grow Cu and ZnO coatings on the Pinus sylvestris var mongolica wood veneer surface [3]. The composites were prepared by d-Ti_3C_2Tx and wood and it had good mechanical properties and electromagnetic shielding effectiveness which was up to 39.3 dB at 12.4 GHz [4]. Wang [5] developed wood-Cu composite materials whose electromagnetic shielding efficiency up to 60 dB. Gu[6] developed a composite material with Ti_3C_2Tx and wood, and its electromagnetic shielding effectiveness can reach 71.3 dB. The carbon fiber/wood fiber/polyacrylamide composite was prepared with the electromagnetic shielding effectiveness of 41.1 dB [7]. Chen used graphene modified carbon fiber to modify wood-plastic composites to explore their EMSE. The EMSE of modified composites was 29 dB from 8.2 GHz to 12.4 GHz [8]. Lou [9] synthesized magnetic wood with excellent adjustable electromagnetic properties by vacuum/pressure impregnation method. Li Yanjun [10] prepared wood and polyaniline composites with electromagnetic shielding via in-situ polymerization

method. The EMSE of the composites was between 30 dB and 60 dB. Feng Yuezhan[11] used magnetic Ni particles modified graphene oxide and nanocellulose to prepare electromagnetic shielding films. The EMSE of magnetic films can reach 32.2 dB (X band). Zhang Xuefeng [12] prepared a composite material using wood and metal Ni. The material was thin, low density and showed excellent EMSE. The EMSE could reach 50.8 dB ranging from 8.2 to 12.4 GHz. Sun [13] used waste sawdust to recycle and it had ideal performance in certain corrosive environments comparing with metal materials. Furthermore, the composites exhibited a conductive and electromagnetic shielding effect.

However, how to conduct the electroless Cu and Ni deposition on wood surface and how to obtain the ideal EMSE of wood-based composites. In addition, whether the electroless Ni would affect the deposition morphology of metal Cu on wood surface.

In this study, electroless Cu and electroless Ni were conducted on wood surface. One time electroless Ni deposition, two times electroless Cu deposition and two times electroless Cu deposition, one time electroless Ni deposition were carried out, respectively. Wood metal composites were prepared by the deposition sequence electroless Cu and Ni and time of electroless Ni, so as to analyze the change rule of electromagnetic shielding performance of wood-based Cu-Ni composites.

Materials And Methods

2.1 Materials

$CuSO_4 \cdot 5H_2O$ 53 g/L, $NaKC_4H_4O_6 \cdot 4H_2O$ 13 g/L, EDTA-2Na 27 g/L, $K_4Fe(CN)_6 \cdot 3H_2O$ 1.3 g/L, Formaldehyde 70 mL/L, $NiSO_4 \cdot 6H_2O$ 33 g/L, $NaH_2PO_2 \cdot H_2O$ 28 g/L, $Na_3C_6H_5O_7 \cdot H_2O$ 30 g/L, CH_4N_2S 10 mg/L and Ammonia 30 mL/L, were analytically pure and bought in Tianjin Beilian Fine Chemicals Development Co., Ltd. The base fluid is deionized water.

Poplar is base material from Tumote Left Banner, Hohhot, 5 years old. Spin cut into veneer, thickness (1.5 ± 0.1) mm, moisture content is about 11.2 %.

2.2 Substrate pretreatment

Immerse of poplar sheet in deionized water for 30 min and cut into sizes of 11.0 cm in diameter. Then put it in a beaker with distilled water and soak it in boiling water at 100°C for 3 h.

2.3 Electroless Cu and Ni

The greased and polished wood is activated in an activation solution [14], then according to $CuSO_4 \cdot 5H_2O$ 53 g/L, $NaKC_4H_4O_6 \cdot 4H_2O$ 13 g/L, EDTA-2Na 27 g/L, $K_4Fe(CN)_6 \cdot 3H_2O$ 1.3 g/L and HCHO 70 mL/L, weigh in proportion and stir evenly in 300 mL deionized water to prepare electroless solution. Adjust the solution with pH = 11.8 (the acidity calibration with 25 % NaOH solution) and temperature 60 ° C, remove activated wood into it and start plating for 12 min. In the meantime, electroless Ni solution was prepared and $NiSO_4 \cdot 6H_2O$ 33 g/L, $NaH_2PO_2 \cdot H_2O$ 28 g/L, $Na_3C_6H_5O_7 \cdot H_2O$ 30 g/L, CH_4N_2S 10 mg/L proportional weight,

stir evenly in 300 mL deionized water, pH = 9 (adjusted with 30 mL/L ammonia) and temperature 60°C. Take out the electroless Cu plated wood and put it into it for 20 min, 25 min, 30 min, 35 min and 40 min. The schematic diagram of composite preparation was shown in Fig. 1.

Electroless Cu and Ni on wood surface in accordance with Table 1. Firstly electroless Cu and then electroless Ni, wood of electroless Cu needed activation treatment. However, firstly electroless Ni and then electroless Cu, wood of electroless Ni didn't need activation treatment.

Table 1
Experimental design scheme

Type	1 time electroless Ni deposition	2 times electroless Cu deposition
1 time electroless Ni deposition	/	1–2
2 times electroless Cu deposition	2 – 1	/

In Table 1, 2 – 1 showed the wood was treated via two electroless Cu deposition and one electroless Ni deposition while 1–2 demenstrated the wood was treated via one electroless Ni deposition and two electroless Cu deposition.

Table 2
Surface roughness of wood based composites

Type	1–2	2 – 1
Ra	4.61 μm	3.45 μm
Sa	12.9 μm	9.99 μm

2.4 Characterization techniques

2.4.1 VK-X160 laser scanning confocal microscope test

Select the object lens for 20 times observation, after the image focus is completed, click on more measurement methods, select the surface measurement method, frame the whole plane, measure its surface roughness, and save data. Then click the 3D test effect diagram to observe the flatness of the coating on the wood chip and select the metal mode. Adjust the viewing angle so that it can fully see the coating surface morphology and save jpg format pictures. Repeat the above observation steps, each sample measured 5 different locations, each position selected 5 different points, save all required measurement data, calculating the average. The size of laser scanning confocal microscope and well depth map is the same as that of 3D image, and the unit is μm.

2.4.2 SEM

The dried samples were prepared and then placed in the sample area to be tested. The surface morphology was analysed via Phenom scanning electron microscopy system.

2.4.3 XRD-6000 x-ray diffraction test

The wood samples treated by electroless plating were dried in a vacuum oven at 30–35°C for 8 h, and then cut into the required size of the mold for measurement. The scanning angle was from 5 to 80°, and the scanning speed was 3 (deg/min).

2.4.4 RTS-8 four-probe tester test

The round thin composites was set on the test platform, and the probe contact sample was slowly adjusted. After the probe contacted the sample, the thin-layer square resistance was selected to conduct the measurement. A coated Ni sample needs to be measured at 5 different positions of the transverse and parallel lines, and 5 different points are taken at each place. The resistance is measured and the average value is taken.

2.4.5 Hydrophobic test

The dry samples were taken, prepared and placed in the sample area to be tested. The contact angle of the material surface was measured by JY-PHa and JYSP-180 contact angle measuring instruments. Each test sample was tested after 30 s of dripping.

2.4.6 DR-S02A Electromagnetic Shielding Test

EMSE of composite materials in L band ranging from 0.3 × 103 to 3.0×103 MHz was tested via DR-SO2A EMSE instrumentation system (Beijing Dingrong Technology Co., Ltd, China). Using ASTM 4935 − 2010 international standard test. Sample thickness is less than 10 mm. The error is + 0.5 dB to -0.5 dB, the maximum VSWR is < 1.2 and insertion loss (IL) ≤ 0.5dB. When the EM waves are incident on the material surface, they can be mostly attenuated by surface reflection, the multiple internal reflections and absorption from the material [15]. According to Schelkunoff's theory, the total EMI SE (SET) is defined as the sum of reflection (SER), multiple reflections (SEM) and absorption (SEA), and expressed as [16–18]:

$$SE_T(dB) = SE_R + SE_M + SE_A \quad (1)$$

$$SE_R(dB) = -10\log(1 - S_{11}^2) \quad (2)$$

$$SE_A(dB) = -10\log\left(\frac{S_{12}^2}{1-S_{11}^2}\right)$$

S_{11} and S_{12} are the measured scattering parameters [15]. The SE_M can be neglected when the SE_T > 15 dB and it can be described as [15]:

$$SE_T(dB) = SE_R + SE_A \quad (4)$$

Results And Discussion

3.1 Surface morphology

The morphology of electroless composite coating on wood surface was shown in Fig. 2. Figure 2a showed that the wood surface was first treated by electroless Ni for one time deposition, and then treated by electroless Cu for two times deposition. A uniform red layer coated the surface, and the red layer was unevenly distributed in the well depth map. In Fig. 2b, the metal layer on the surface of wood was arranged along the inherent wood grain to form a banded metal layer and there was a certain height difference between the banded layers. At this time, the surface roughness of the composite coating was 12.9 μm, and the linear roughness was 4.61 μm, which was shown in Table 2. Figure 2c showed that the wood surface was firstly treated by two times electroless Cu, and then one time electroless Ni deposition. The surface was covered with a uniform silver-gray coating, which was evenly distributed in the well depth map. In Fig. 2d, the distribution of metal layer on the surface of wood was still arranged along the inherent wood grain to form a banded metal layer, and there was a certain height difference between the banded layers. At this time, the surface roughness of the coating was 9.99 μm and the line roughness was 3.45 μm (Table 2). After electroless Cu, fine Cu particles can fill the inherent porous structure of wood and promote the formation of uniform metal layer on wood surface. In the meantime, uniform Cu layer provided an ideal self-catalytic substrate for the deposition of Ni particles. Therefore, firstly electroless Cu on the wood surface and then electroless Ni, the formed composite coating had relatively flat surface, and the linear roughness and surface roughness were ideal.

3.2 SEM Analysis

The SEM morphology of electroless composite coating on wood surface was shown in Fig. 3. Figure 3a showed that many smaller particles were distributed on the surface of wood, and local particles aggregated together. The larger particles in Fig. 3b closely covered the wood surface and had a larger pore structure locally. Figure 3c was a local enlarged view of Fig. 3a. It can be seen that Cu particles grew closely among Ni particles and embedded in Ni particles, indicating that there was no exposed wood, which proved that the wood was completely coated by Cu and Ni. Figure 3d and 3e showed that after electroless Cu and Ni treatment on wood surface, the surface coating was not only uniform but also had a large thickness. The thickness of the former coating was 157 μm, while that of the latter coating was 84 μm (Table 3). Due to the large size of Ni particles, the surface of the deposited wood was not fully covered by the inherent defects of the wood, and some particles will fill this part of the defects in the process of Cu particle deposition, resulting in the uniformity of the composite coatings. In addition, the difference of coating thickness on wood surface proved that the uniformity of substrate surface would directly affected the deposition thickness and uniformity of coating, which further restricted the self-catalytic reaction rate of coating. At the same time, the corrosion degree of the composite substrate was relatively large when the wood was electroless Cu and then electroless Ni deposition. The difference of composite interface substrate verified that the acidity condition of electroless Ni was easier to dissolve wood components. However, the magnification of the coatings in Fig. 3e showed that the Cu coating was uniformly deposited on the Ni layer surface, and the deposition Ni followed by deposition Cu had no effect on the composite coatings.

Table 3
Surface roughness of wood based composites

Type	Wood thickness (μm)	Thickness of composite (μm)	Coatingsthickness (μm)
1–2	308	392	84
2 – 1	198	355	157

3.3 XRD Analysis

The relationship between the electroless Cu-Ni treatment on different wood surfaces and the crystalline properties of the coatings was shown in Fig. 4. The crystal patterns of the samples were obtained by electroless Ni once before electroless plating Cu twice and electroless Cu two times before electroless Ni one time deposition. Figure 4a showed that the diffraction peaks at 2θ = 43, 50.54 and 74.44° were face-centered cubic structures Cu (111), (200) and (220), respectively [19]. The diffraction peak at 2θ = 44.5° was the characteristic peak of the face-centered cubic structure Ni (111) [20];In Fig. 4b, the intensity of the diffraction peak at 2θ = 53 ° had a local change [21], which may be due to the mutual extrusion of the Cu and Ni coatings on the wood surface Fig. 4c showed that the diffraction peak of Ni (220) had disappeared at 2θ = 78°, and the diffraction peak of Cu (220) had split at 2θ = 74.44°, which further proved that the metal Cu and Ni were tightly embedded together to form a dense composite layer. It can be concluded that the metal Cu and Ni on the wood surface were tightly embedded together, and the dense composite layer would refine the grain size of the wood surface composite.

3.4 Hydrophobic performance Analysis

The comparison of hydrophobicity of electroless coatings on wood surface was shown in Fig. 5. The figure marked 1 was the hydrophobic of wood surface by electroless Ni one time before plating Cu two times, and the figure marked 2 was the hydrophobic by electroless Cu two times before plating Ni one time. The contact angle of the former was 107.8° by three-point method and the latter reached 122.5 °. The surface of Cu block was smooth, and the contact angle was generally below 90° [21]. Similarly, the contact angle of Ni surface was also less than 90° indicating that they were hydrophilicity [22]. However, the composites via electroless Ni and Cu were hydrophobicity, and the composites via two electroless Cu depositions and one electroless Ni deposition showed better hydrophobicity. The reason was that the surface of wood was deposited by Cu layer twice and then Ni layer was deposited. Because of the smaller Cu particles, the inherent defects of wood surface were well filled. The metal Cu and Ni were tightly embedded together to form a dense and thick composite metal layer, which can avoid the penetration of water molecules and improve the hydrophobic effect of the composite coating.

3.5 Conductivity Analysis

Figure 6 was the electrical conductivity of composites with different treatment conditions, the data showed that the conductivity of the composite increased gradually with the extension of electroless Ni time. The conductivity of labelled 1–2 curve changed obviously. When the electroless Ni time was 25 min

and 35 min, the conductivity curve showed inflection points. The conductivity of labelled 2 – 1 curve fluctuated greatly with time. After two times of electroless Cu and one time of electroless Ni, the electrical conductivity of the composite was small and controllable, and the average conductivity along the grain reached 2370.76 S/cm. The conductivity of coatings via electroless Ni and electroless Cu was showed in Table 4. The possible reason was that the porous structure of wood, the metal Cu deposited on the surface of wood filled the inherent defects, and the deposition again of metal Ni on the surface of Cu layer would promote its distribution to be more uniform. Because Ni particles were large, there were gaps at the contact interface, and gas phase may exist in the gap, which affects its conductivity.

Table 4
The conductivity of coatings via electroless Cu and electroless Ni

Type	Conductivity (S/cm)
One time electroless Ni deposition	258.15
Two times electroless Ni deposition	316.51
One time electroless Cu deposition	509.14
Two times electroless Cu deposition	1984.95

3.6 Electromagnetic shielding effectiveness Analysis

Figure 7 and Table 5 showed that different electroless Ni and Cu treatments on the wood surface, the EMSE of the composites presented different trends ranging from 300 KHz to 3.0 GHz. After two times electroless Cu and one time Ni deposition, the EMSE of the composite increased firstly and then decreased. When the deposition Ni time was up to 25 min, the EMSE of the composite was better, with an average value of 93.8 dB. After one time electroless Ni and two times Cu deposition, the electromagnetic shielding effectiveness of the composite increases first and then decreases. When the electroless Nitime was 30 min, the electromagnetic shielding effectiveness of the composite was better, with an average value of 75.8 dB. The above analysis verified that the composite prepared by electroless Cu firstly and then Ni layer had good EMSE.

Table 5
The relation between the order of deposition and electromagnetic shielding effectiveness

Type of deposited coatings	electromagnetic shielding effectiveness (dB)
1–2 (20 min)	72.6
1–2 (25 min)	73.3
1–2 (30 min)	75.8
1–2 (35 min)	72.7
1–2 (40 min)	69.2
2 – 1 (20 min)	92.6
2 – 1 (25 min)	93.8
2 – 1 (30 min)	86.7
2 – 1 (35 min)	90.5
2 – 1 (40 min)	86.3

Figure 7 showed that the EMSE of composites was not proportional to the conductivity. Figure 6 showed that the conductivity of the standard 1–2 was twice that of the standard 2 – 1, but the electromagnetic shielding effectiveness was 20 dB different. The comparison between Fig. 8a and Fig. 8c showed that the type 2 – 1 of composites had stronger electromagnetic wave absorption ability and the type 1–2 of composites had stronger electromagnetic wave reflection ability (Fig. 8c and Fig. 8d). Due to the good impedance matching, the incident electromagnetic wave can easily penetrate the interior of the composite coating, and only a few electromagnetic waves can be reflected. The absorption layer with positive conductivity gradient and negative magnetic gradient achieved strong electromagnetic absorption through strong hysteresis loss and dielectric loss [23]. Strong hysteresis loss was the main electromagnetic wave loss mode.

Electroless Cu and Ni coatings on wood had synergistic effect on electromagnetic shielding effectiveness, mainly due to separation of conductive network and specific interface polarization mechanism of composite coatings [24–25]. The desired conductive network of composites would show superior charge storage capacity and promote absorption of more incident electromagnetic microwave energy by polarization of electric field [23–26].

It was obvious that the SE_T value was up to 93.8 dB and effective absorption value of 0.9999 at 3 GHz, indicating that the multilayer composites can block over 99.99% of incident EM waves [23–26].

It should be noticed that the SE_T increased first and then decreased with increasing the conductivity, which is different from the previous reports where a higher conductivity will cause a higher SET. On the

contrary, both the values of SE_T and SE_A exhibited an increasing trend with the increase of magnetic permeability [27].

3.7 Hydrophobic property of electroless Ni time

The above analysis verified that the composite coating with electroless Cu twice and electroless Ni once on the wood surface had good hydrophobicity. In order to further study the hydrophobic properties of the composite coating, which were compared by selecting six treatment times of electroless Ni for 35 min, 40 min, 45 min, 50 min, 55 min and 60 min. Figure 9 was the surface contact angle test diagram of wood-based metal composites after electroless Cut wice and then electroless Ni once. Figure 9a, b, c, d, e and f were the treated samples with different electroless Ni time, respectively, 35 min, 40 min, 45 min, 50 min, 55 min and 60 min. The data showed that the contact angles of wood-based composites were 112.2, 114.6, 121.6, 122.5, 123.0 and 114.0° (Table 6). When the deposition Ni time was up to 55 min, the hydrophobic property was the ideal. Here, the contact angle was 123.0°.

Table 6
The contact angle of electroless Cu/Ni composites

Electroless Ni time (min)	contact angle (°)
35	112.2
40	114.6
45	121.6
50	122.5
55	123.0
60	114.0

The reason was that the metal layer coated on the wood surface, which would promote the self-catalytic reaction rate and prolong the electroless Ni time. The roughness of the metal layer decreases gradually. The smoothness of the coating surface tended to be uniform and the particles tended to be close. The small Cu particles can make up for the inherent defects of the wood. The Ni particles grown up on the surface of the uniform Cu layer, and the metal layer structure on the wood surface was dense. Therefore, the hydrophobic property of the composites was best.

3.8 Formation mechanism of composite coatings

Microscopically, wood had inherent characteristics with micro/nano multi-scale pore structure, and its natural skeleton morphology can be used as matrix templates for other materials [28]. In this study, the surface pores of wood would increase after degreasing treatment. A part of Cu element was deposited on activated pores and wood surface during electroless Cu, then Ni layer was deposited on Cu layer by electroless again. The data of electromagnetic shielding effectiveness (Table 5) showed that the conductive composite obtained by firstly electroless Cu then electroless Ni had ideal electromagnetic

shielding effectiveness [29]. Electromagnetic waves went through multilayer composites, and a large amount of free charge accumulated spontaneously between the metal layer and the wood [30], three Ni/Cu Cu/Cu Cu/Wood layers with different electrical–magnetic properties can induce multiple reflections at each interface, which promote to the absorption attenuation [23]. Figure 3b demonstrated that the microstructure of nickel grains is coral-like, and there are many space and pores between the nickel particles, which increased the multiple reflection and absorption effects of the incident electromagnetic waves between them [30]. In addition, due to the inherent porous structures, the Cu-Ni coatings were also endowed with 3D cell structure, as depicted in the Fig. 10 [30]. The electromagnetic waves was reflected and scattered repeatedly within the porous metal coatings and was significantly attenuated by reflection loss and dielectric loss [31–33]. At the same time, using this efficient multilayer structure, multiple reflection and absorption of incident electromagnetic microwave between Cu and Ni layers are carried out [30].With the extension of electroless Ni time, metal Cu and Ni were tightly embedded together. Cu layer and Ni layer squeezed each other to form a dense composite layer, which had good electromagnetic shielding effectiveness. The formation mechanism of electroless Cu-Ni composite coating on wood surface was shown in Fig. 10.

Conclusions

(1) The electrical conductivity along grain could reach 2953.64 S/cm and the thickness of wood-based composite coating can be up to 157 μm via two electroless Cu depositions and one electroless Ni deposition deposition.

(2) The surface roughness could reach 9.99 μm, and the line roughness was 3.45 μm.

(3) XRD showed that the surface metal Cu and Ni of wood were tightly embedded together to form a dense composite layer.

(4) When the deposition Ni time was up to 55 min, the hydrophobic property of the multilayer composites was the ideal. Here, the contact angle was 123.0°.

(5) The average electromagnetic shielding effectiveness of Cu and Ni wood-based composites can reach 93.8 dB at L band ranging from 0.3×10^3 to 3.0×10^3 MHz with a low thickness (157 μm), verified the multilayer composite materials can block over 99.99% of incident EM waves.

Declarations

Disclosure statement

No potential conflict of interest was reported by the authors.

Funding

This work was supported by Natural Science Foundation of Inner Mongolia Autonomous Region (2019BS03014 and 2018BS02003), the Start-up Project of Inner Mongolia Agricultural University High-level Talents Introduction Scientific Research (NDYB2016-24), The Colleges and Universities Science Research Project of Inner Mongolia Autonomous Region (NJZY18058 and NJZY21468), Science research innovation projects of the Inner Mongolia Agricultural University for undergraduate (KJCX2020025) and Science and Technology Innovation Leading Project of Inner Mongolia Autonomous Region (KCBJ2018013), The undergraduate innovation and entrepreneurship training program (202110129007).

References

1. W.M. Bulleit, Reinforcement of wood materials: a review. Wood fiber sci **16**(3), 391–397 (1984)
2. Y. Chai, F. Fu, S.Q. Liang, Research progress of wood-based metal functional composites. Journal of Beijing Forestry University **41**(3), 151–160 (2018)
3. J.K. Li. Preparation and physical properties of nano-Cu/ZnO coated wood matrix composites [dissertation]. Haerbin: Northeast Forestry University; 2019
4. Z.X. Wang, X.S. Han, J.W. Pu et al., Mxene/wood-derived hierarchical cellulose scaffold composite with superior electromagnetic shielding. Carbohydr. Polym. **254**, 117033 (2021)
5. L.J. Wang, L.L. Sun, J. Li, Electroless copper plating on fraxinus mandshurica veneer using glyoxylic acid as reducing agent. BioResources **6**(3), 3493–3504 (2010)
6. C.B. Liang, H. Qiu, J.W. Gu, Ultra-light mxene aerogel/wood-derived porous carbon composites with wall-like mortar/brick structures for electromagnetic interference shielding. Sci Bull **65**, 616–622 (2020)
7. B.K. Dang, Y.P. Chen, Q.F. Sun et al., Effect of carbon fiber addition on the electromagnetic shielding properties of carbon fiber/polyacrylamide/wood based fiberboards. Nanotechnology **29**, 1–9 (2018)
8. J. Chen, Z.Y. Teng, Y.Y. Zhao et al., Electromagnetic interference shielding properties of wood-plastic composites filled with graphene decorated carbon fiber. polym composit **39**(6), 2110–2116 (2018)
9. Z.C. Lou, H. Han, M. Zhou et al., Synthesis of magnetic wood with excellent and tunable electromagnetic wave absorbing properties by a facile vacuum/pressure impregnation method. ACS Sustain. Chem. Eng. **6**(1), 1000–1008 (2018)
10. W. He, J.P. Li, Y.J. Li et al., Characteristics and properties of wood/polyaniline electromagnetic shielding composites synthesized via in situ polymerizationp. Polym composit **39**(2), 537–543 (2018)
11. G.J. Han, Z.G. Ma, Y.Z. Feng et al., Cellulose-based Ni-decorated graphene magnetic film for electromagnetic interference shielding. J. colloid interface Sci **583**, 571–578 (2021)
12. Y. Zheng, Y.J. Song, X.F. Zhang et al., Lightweight and Hydrophobic Three-Dimensional Wood-Derived Anisotropic Magnetic Porous Carbon for Highly Efficient Electromagnetic Interference Shielding. ACS Appl Mater Interfaces **12**, 40802–40814 (2020)

13. X.L. Zhu. Multi-scale electrical performance simulation of carbon fiber reinforced wood matrix composites [master's thesis]. Haerbin: Northeast Forestry University; 2016
14. Y.F. Pan, D.W. Yin, J.T. Huang et al., Performance and preparation of the electroless Ni wood-based composites. BioResources **15**(4), 7517–7531 (2020)
15. W. Yang, B. Shao, T. Liu et al., Robust mechanically and electrically self-healing hydrogel for efficient electromagnetic interference shielding. ACS appl mater interfaces **10**, 185–195 (2018)
16. H.B. Zhang, Q. Yan, W.G. Zheng et al., Tough graphene-polymer microcellular foams for electromagnetic interference shielding. ACS appl mater interfaces **3**, 918–924 (2011)
17. C.M. Watts, X. Liu, W.J. Padilla, Metamaterial electromagnetic wave absorbers. Adv Mater **24**, OP98–OP120 (2012)
18. Y. Zhan, J. Wang, K. Zhang et al., Fabrication of a flexible electromagnetic interference shielding Fe3O4@reduced graphene oxide/natural rubber composite with segregated network. Chem. Eng. J. **344**, 184–193 (2018)
19. T.C. Guo, Y. Wang, J.T. Huang, Studies of electroless copper plating on poplar Veneer. BioResources **11**(3), 6920–6931 (2016)
20. Y.F. Pan, X. Wang, J.T. Huang, The preparation, characterization, and influence of multiple electroless Nickel-Phosphorus (Ni-P) composite coatings on poplar veneer. BioResources **11**(1), 724–735 (2016)
21. A. Sheng, W. Ren, Y.Q. Yang et al., Multilayer WPU conductive composites with controllable electro-magnetic gradient for absorption-dominated electromagnetic interference shielding. Composites Part A **129**, 105692 (2020)
22. Y.B. Tao, P. Li, S.Q. Shi, Effects of carbonization temperature and component ratio on electromagnetic interference shielding effectiveness of wood ceramics. Materials **9**, 540 (2016)
23. J.H. Ha, S.K. Hong, J.K. Ryu et al., Development of multi-functional graphene polymer composites having electromagnetic interference shielding and de-Lcing properties. Polymers **11**, 2101 (2019)
24. N. Yousefi, X.Y. Sun, J.K. Kim et al., Highly aligned graphene/polymer nanocomposites with excellent dielectric properties for high-performance electromagnetic interference shielding. Adv. Mater **26**, 5480–5487 (2014)
25. Y. Wang, W. Wang, X.D. Ding et al., Multilayer-structured Ni-Co-Fe-P/polyaniline/polyimide composite fabric for robust electromagnetic shielding with low reflection characteristic. Journal of Chemical Engineering **380**(12), 108–113 (2020)
26. L. Wang, Z. Wang, G.Y. Ning et al., Research progress of wood-based conductive electromagnetic shielding materials. Mater Report **32**(7), 2320–2328 (2018)
27. Q. Liu, Q. Cao, H. Bi, CoNi@SiO2@TiO2 and CoNi@Air@TiO2 microspheres with strong wideband microwave absorption. Adv Mater. **28**(3), 486–490 (2016)
28. J.W. Li, A.F. Wang, J.B. Qin et al., Lightweight polymethacrylimide@copper/nickel composite foams for electromagnetic shielding and monopole antennas. Compos. A **140**, 106144 (2021)

29. S. Li, Z. Xu, Y. Dong et al., Ni@nylon mesh/PP composites with a novel treering structure for enhancing electromagnetic shielding. Compos Part A: Appl Sci Manuf **131**, 105798 (2020)
30. X. Wang, B. Wen, X. Yang, Construction of core-shell structural nickel@graphite nanoplate functional particles with high electromagnetic shielding effectiveness. Compos Part B: Engineering **173**, 106904 (2019)
31. J. Li, Y. Ding, Q. Gao et al., Ultrathin and flexible biomassderived C@CoFe nanocomposite films for efficient electromagnetic interference shielding. Compos Part B: Eng **190**, 107935 (2020)
32. Z.R. He, X.H. Jie, W.Q. Lian, Hierarchical structure and hydrophobic properties of copper based micro/nano structure prepared by EDM. Mater Eng **48**(01), 144–149 (2020)
33. F.F. Tian, M.A. Hu, M. Li et al., Preparation of superhydrophobic nickel film by electrochemical deposition. Fudan Journal (Natural Science Edition) **51**(02), 163–167 (2012)

Figures

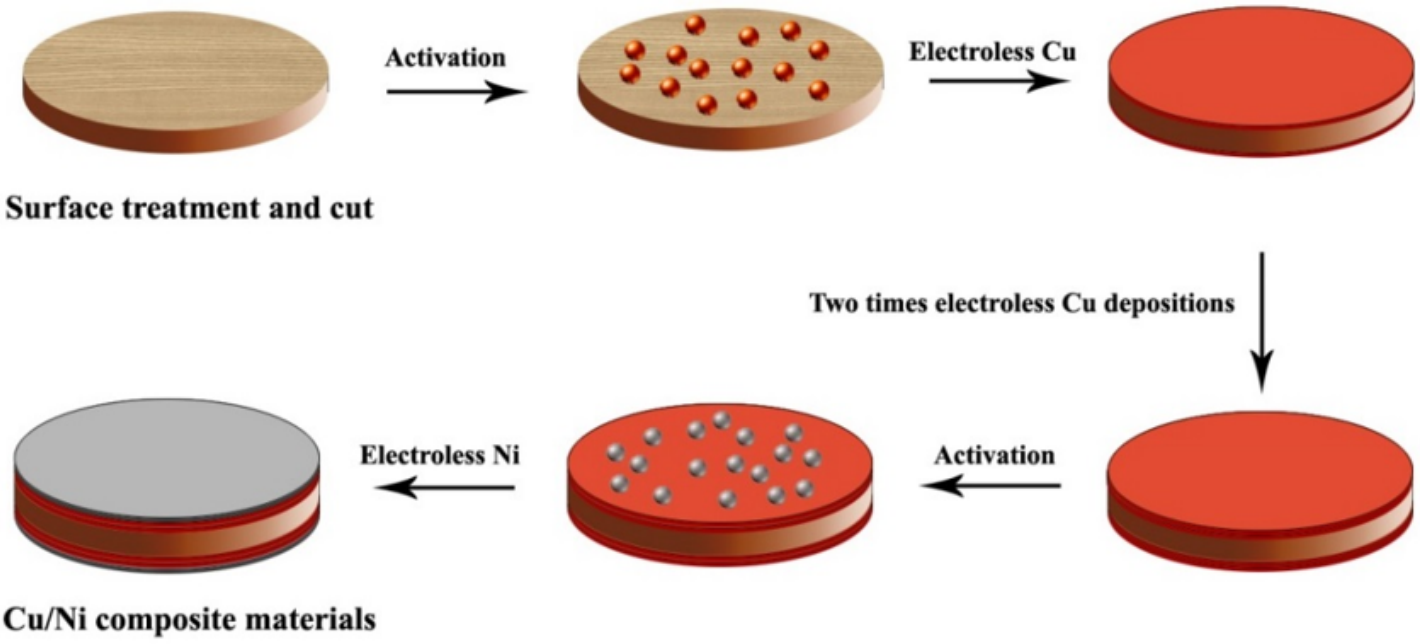

Figure 1

The preparation schematic diagram of electroless Cu-Ni wood based composites

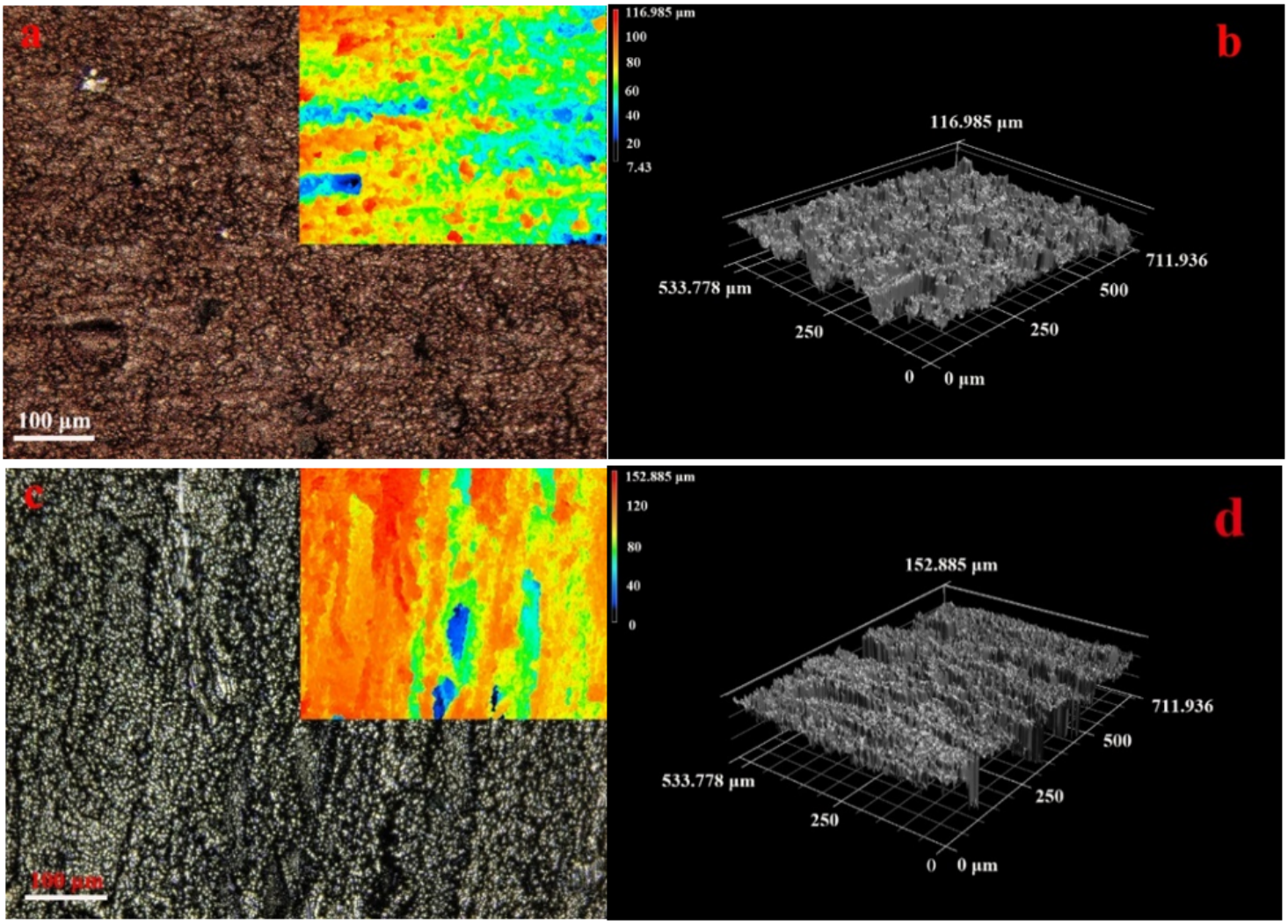

Figure 2

Surface morphology (a: 1-2 surface morphology, c: 2-1 surface morphology, b and d were high image, respectively, electroless time 20 min, inset shows depth map)

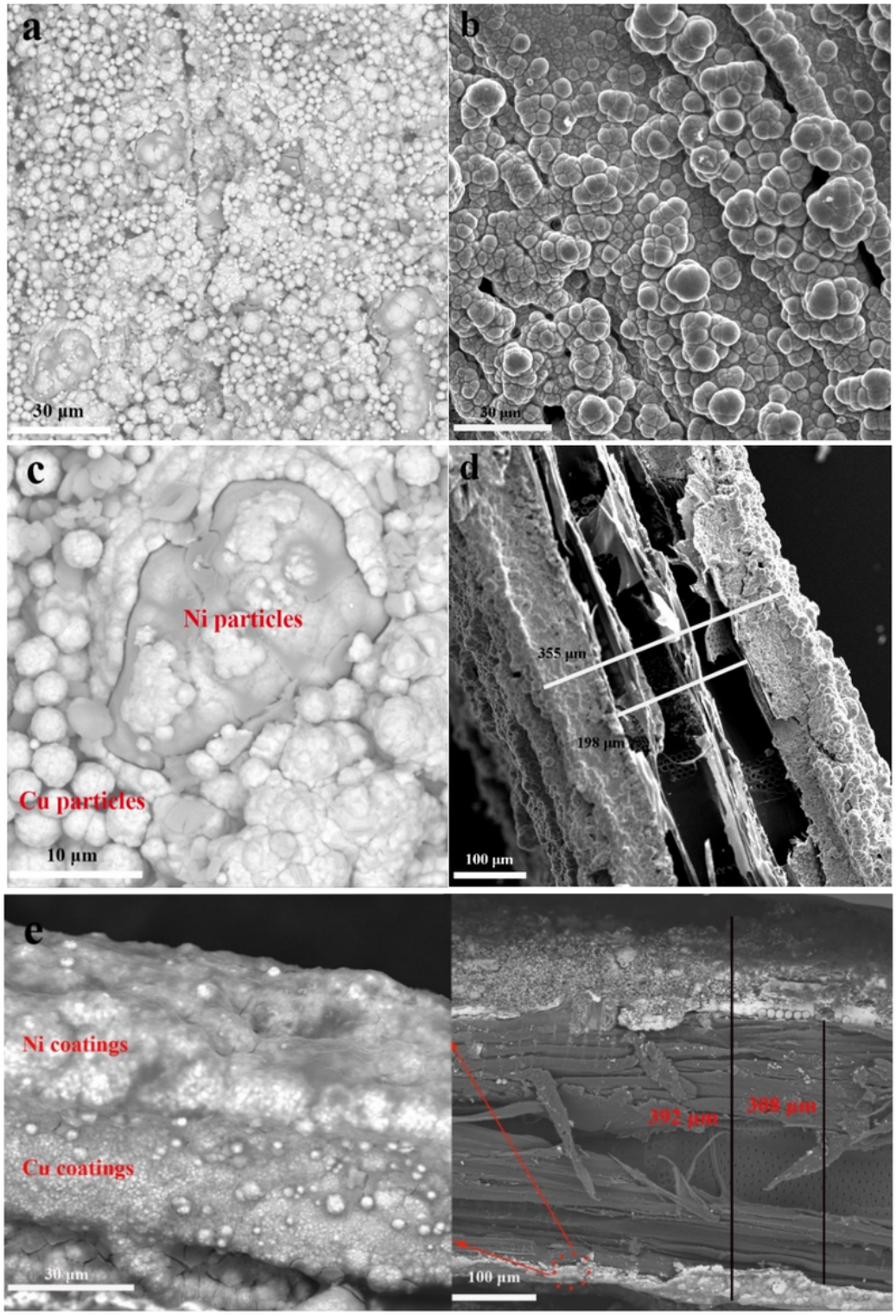

Figure 3

Interface morphology (a and c: 1-2 surface morphology, b: 2-1 surface morphology, d is interface morphology of a and c, e is interface morphology of b)

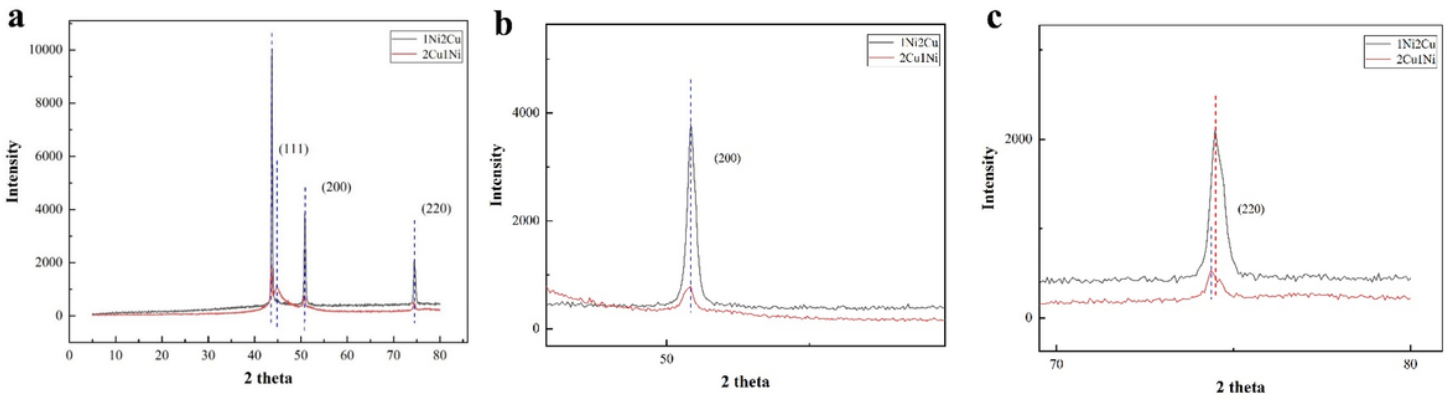

Figure 4

XRD (a full spectrum, b local part enlargement)

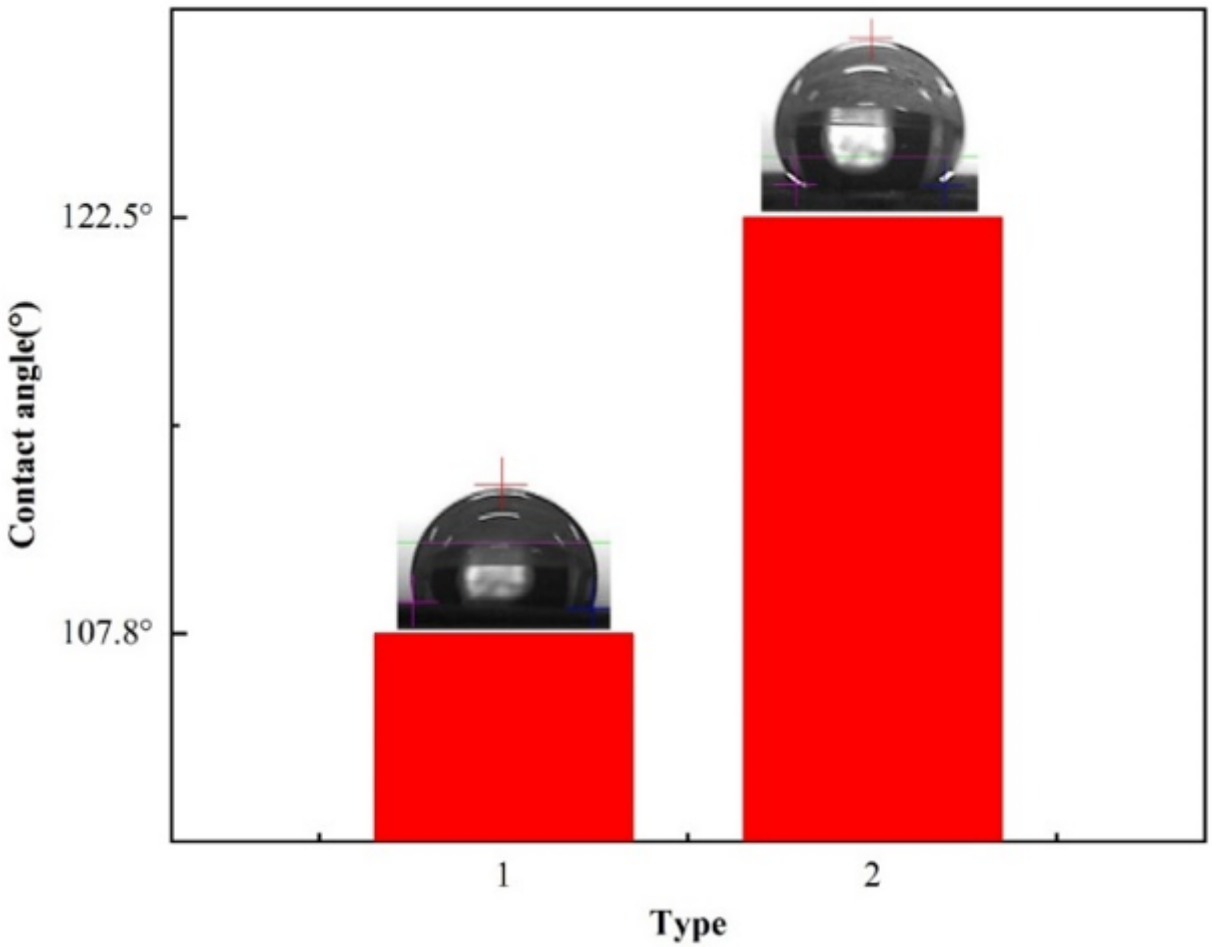

Figure 5

Contact angle (1: 1-2, 2: 2-1)

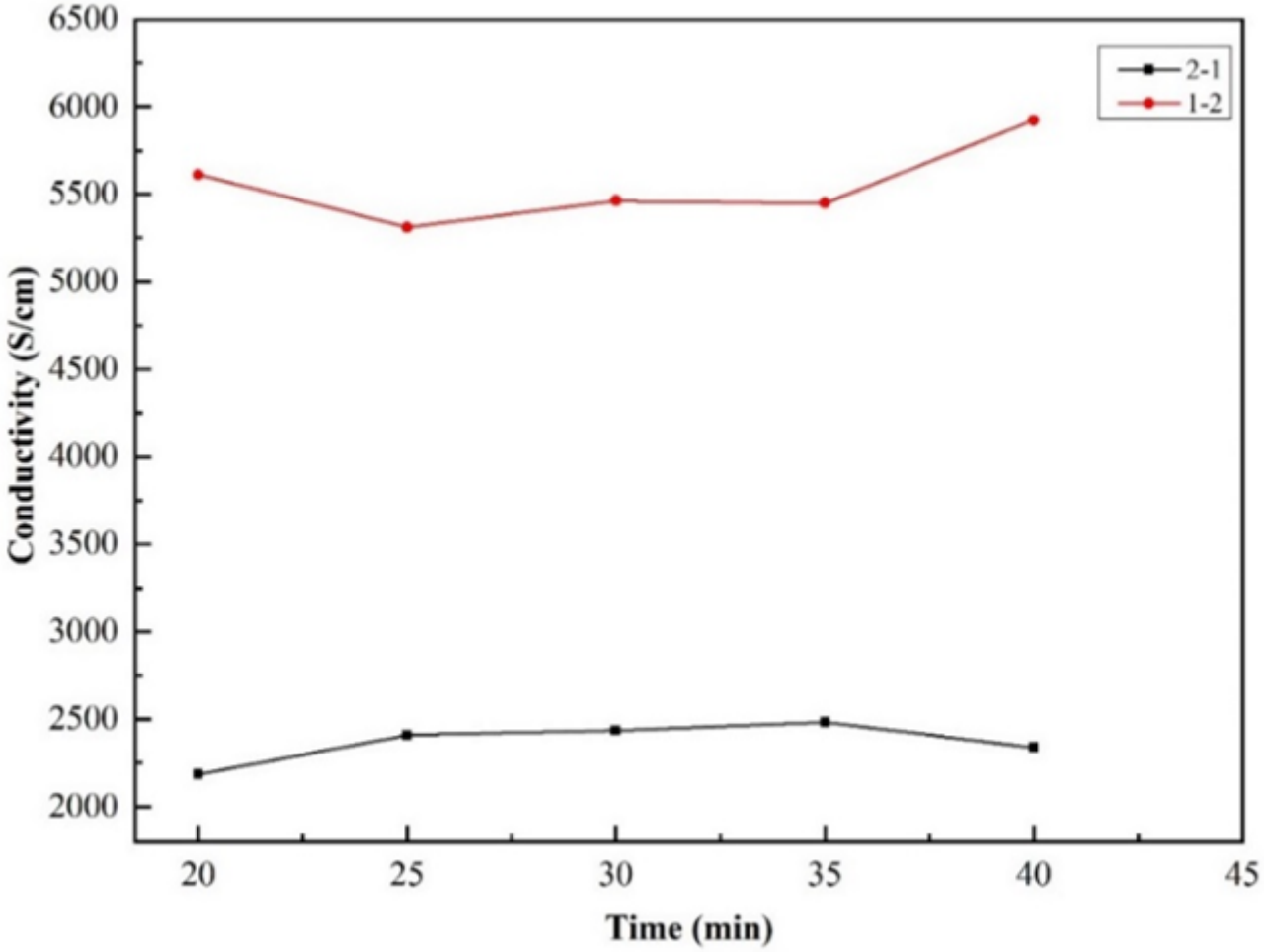

Figure 6

Relationship between conductivity of electroless coatings and electroless time

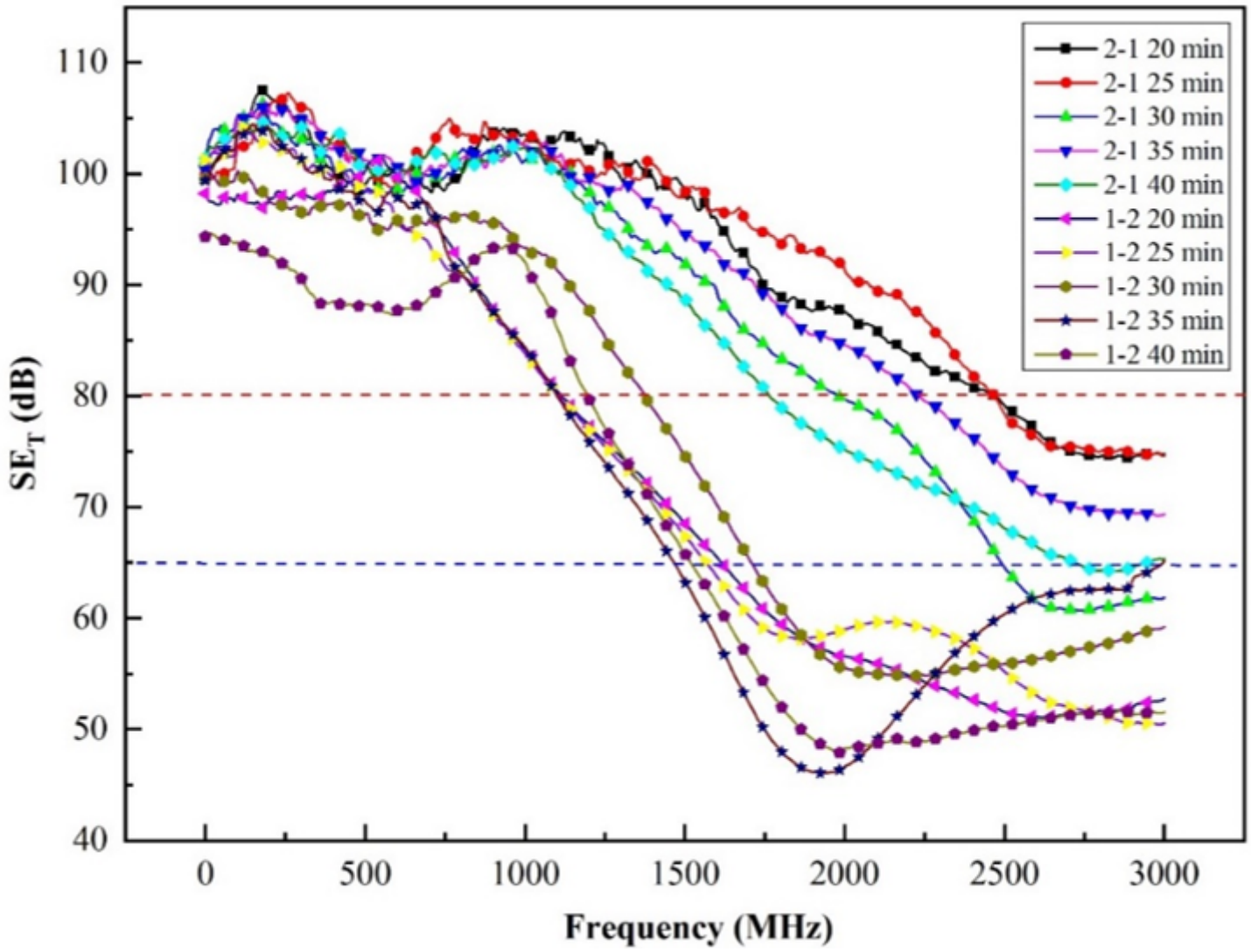

Figure 7

Relationship between electromagnetic shielding effectiveness of coatings and composite plating time

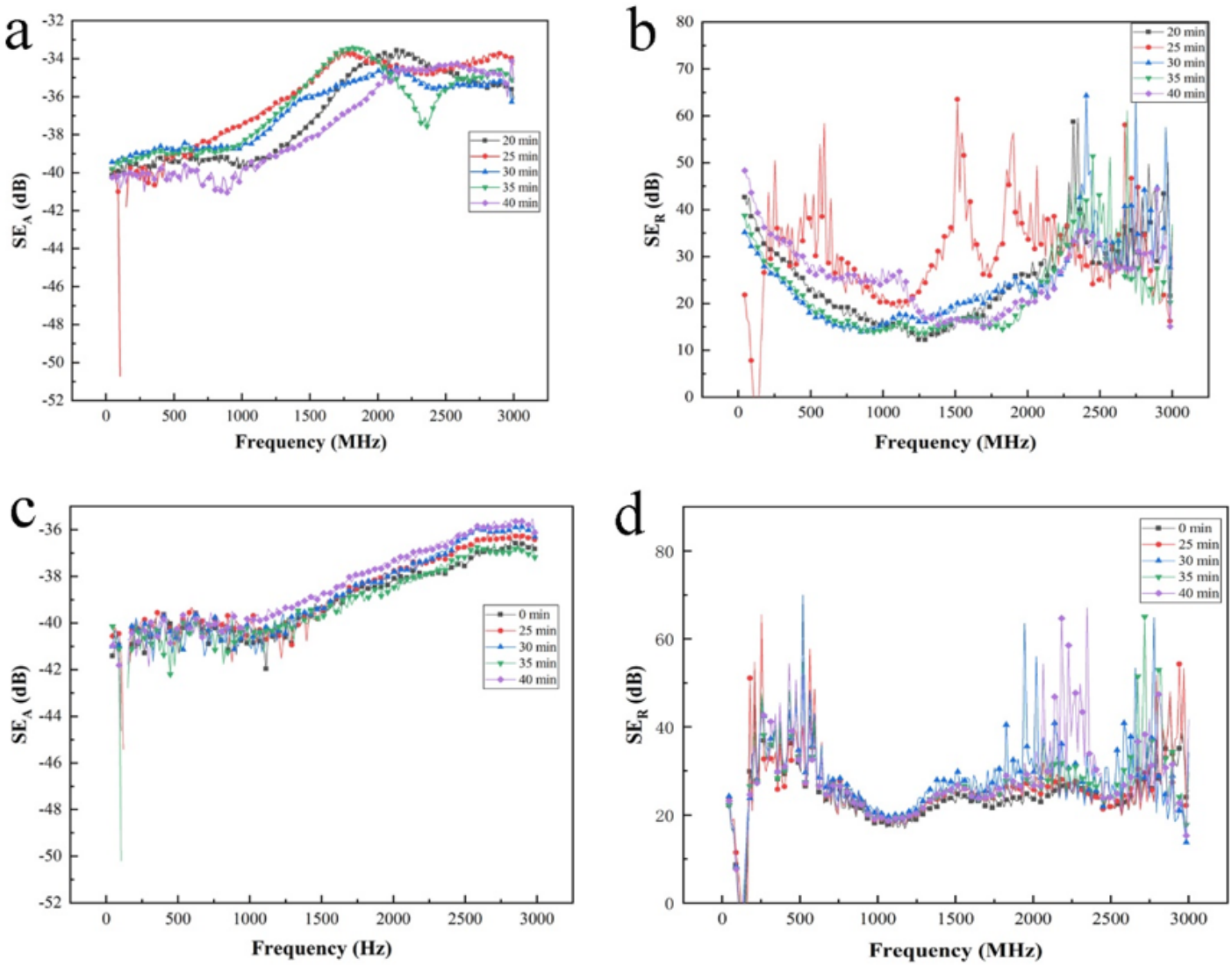

Figure 8

SEA and SER of the samples in the L-band (1-2: a and b, 2-1: c and d)

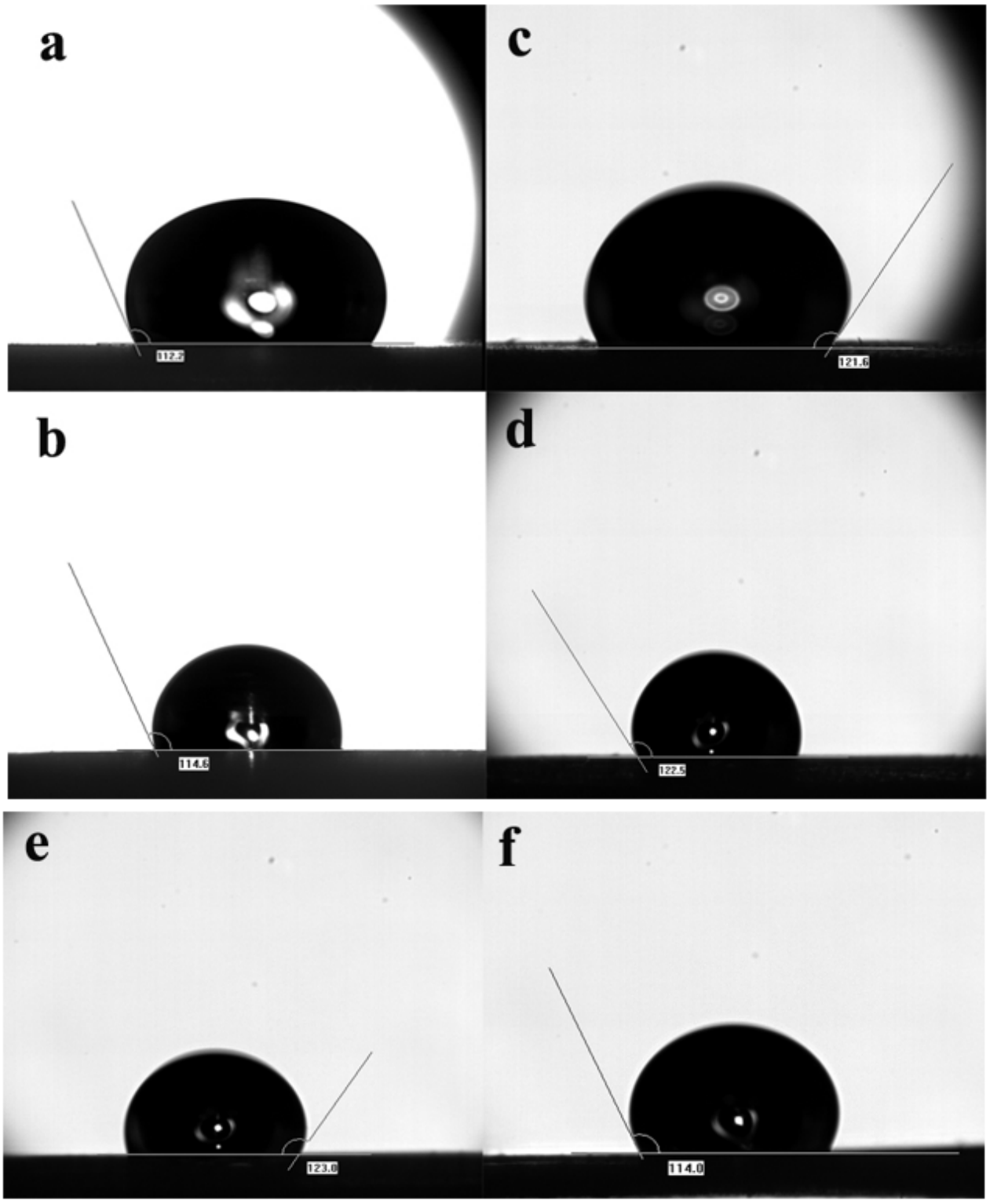

Figure 9

Hydrophobicity performance (a electroless Ni 35 min, b electroless Ni 40 min, c electroless Ni 45 min, d electroless Ni 50 min, e electroless Ni 55 min, f electroless Ni 60 min)

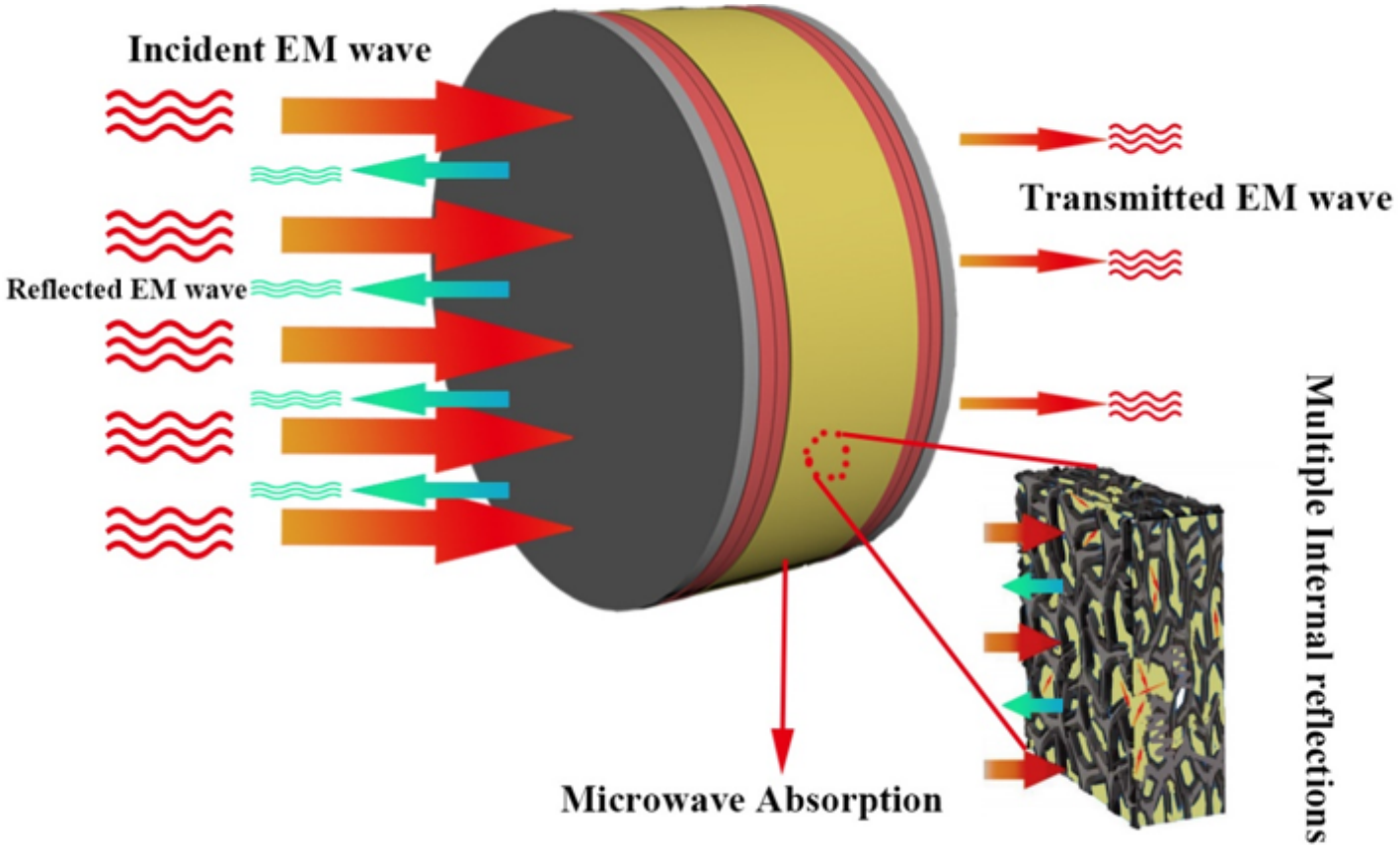

Figure 10

Diagram of formation mechanism of composite coating